Fermi National Accelerator Laboratory

TM-1548

Energy Deposition in TEVATRON Magnets from Beam Losses in Interaction Regions

A. Van Ginneken
Fermi National Accelerator Laboratory
P.O. Box 500, Batavia, Illinois

October 1988

Operated by Universities Research Association Inc. under contract with the United States Department of Energy

ENERGY DEPOSITION IN TEVATRON MAGNETS FROM BEAM LOSSES IN INTERACTION REGIONS

A. Van Ginneken

Fermi National Accelerator Laboratory
Batavia, IL 60510

October 1988

INTRODUCTION

In addition to interacting in the detector, particles produced at an interaction region also deposit energy, with less desirable consequences, in magnets and other components of the accelerator. This note briefly assesses the damage potential of these (essentially unavoidable) beam losses from the viewpoint of quenching of superconducting magnets in an upgraded Tevatron, specifically for the 1 TeV p-$\bar{p}$ option with a luminosity of 10^{31} $cm^{-2}sec^{-1}$, though the results carry more generality. Related issues such as radiation damage to detector electronics or other components are not addressed here. These are thought to be less problematic at the Tevatron, as is thus far supported by operational experience.

Analogy to Extraction Losses

A similar (and actually more serious) situation is encountered in fixed target mode during resonant extraction where unavoidable losses occur when a small fraction of the beam strikes the wires of the electrostatic septum. A detailed analysis, based on reasonably realistic Monte Carlo simulations of these losses, exists[1] and this note relies heavily on that study.

Inelastic interactions in the septum produce a full spectrum of lower energy particles, mostly pions along with some nucleons and kaons. Charged particles with small bending radii disappear quickly from the aperture and a significant fraction of their energy would be deposited in nearby superconducting magnets and, under normal operating conditions, cause a quench. To prevent this a 'dogleg' of four conventional magnets was installed which encompasses the septum and absorbs the major fraction of the energy deposition, thereby shielding the downstream superconducting magnets. The septum is situated between the first and second magnet of the dogleg so that forward created neutral particles are directed away from the superconducting magnets downstream. So-called leading particles with energies in excess of ~70% of the beam energy remain within the dogleg aperture after which they are gradually swept onto the

(radially in-)side of the beampipe wall by the main dipole field. The energy deposited remains significant over a distance of roughly one cell into the lattice. If no further precautions are taken this energy depostion is predicted to be near the quench limit as both beam energy and intensity approach their design goals. This has not yet been subject to verification.

Elastic or quasi-elastic scattered protons are characterized by small energy losses and small angles,[2] which permits them to travel with the beam for considerable distances, though a significant fraction is lost eventually at one or more aperture limiting locations. These losses therefore tend to be more concentrated than the inelastic kind. This is further enhanced because, even at the loss point, the elastics still very much resemble a 'beam' which intercepts the beampipe in the midplane with relatively narrow vertical spread. Quenches in the Tevatron from beam loss due to elastics have been observed and compared with results of simulations. While agreement can only be claimed to be semi-quantitative, this is reasonable in view of a very strong sensitivity to geometric factors such as magnet alignment and position of the closed orbit.

Losses from Interaction Regions

The problem of losses from collisions in the interaction regions can likewise be split into elastic and inelastic parts with p-$\bar{p}$ collisions replacing the interactions of protons with tungsten nuclei (and electrons) in the septum. The elastics can be further divided into (a) multiple Coulomb scattering, summed over repeated beam crossings, and (b) particles having participated in (nuclear) elastic or single diffractive events. The multiple scattering part is treated as a contribution to (slow) transverse beam growth rather than as a beam loss. It is included in this discussion because of its close relationship to the other physical mechanisms. Interference between Coulomb and nuclear scattering is neglected.

INELASTICS

One potential hazard associated with inelastics is quenches in the string of low beta quadrupoles which is positioned close to the center of the interaction region, without the benefit of any shielding. Of lesser concern are neutral particles which travel unimpeded from the interaction region until intercepted by the out-side (i.e., the side away from the center of the ring) of the beampipe-wall ~7 m into the first dipole string. Both cases are Monte Carlo analyzed using an approximate geometry. The neutrals simulation also affords a look at the energy deposition by leading particles.

The inelastic collisions are assumed to take place head on and at the exact center since the x,y-extent of the interaction region is small compared to the beampipe radius and the z-extent is small compared to the distance to the magnets. This assumption also results in a more concentrated energy deposition in the magnets thereby providing useful uppper limits. Simulation of 1 TeV on 1 TeV collisions relies on a simple parametrization of Monte Carlo results of the program DTUJET[3] specifically for this energy. Particle interactions and transport in beampipe, iron ring, and magnets is simulated by CASIM.[4]

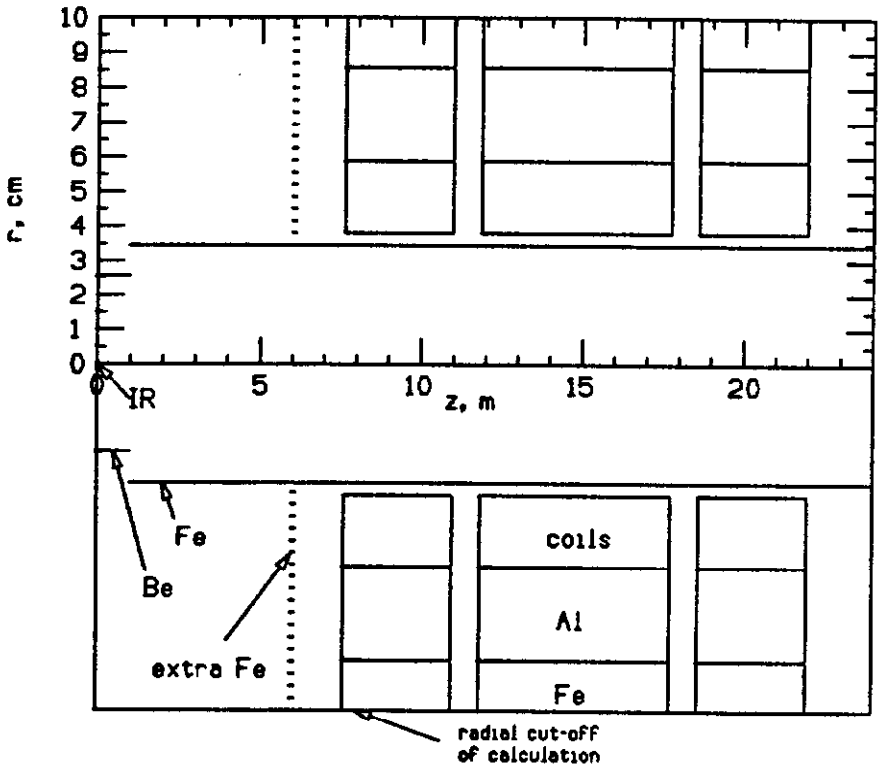

Fig. 1. Overall geometry of interaction region, with low beta quads, as represented in simulation of inelastic interactions.

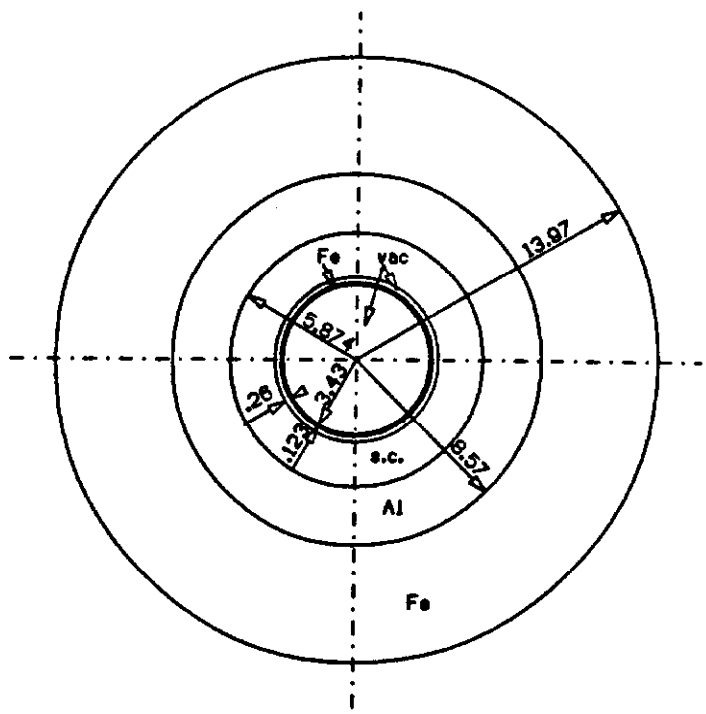

Fig. 2. Cross section of quadrupole magnet as represented in simulation. All dimensions are in cm.

Low Beta Quads

Simulation of the problem of the low beta quads[5] incorporates the overall geometry shown in Fig. 1, with the quads as in Fig 2. A lot of detail is omitted: flanges, valves, detector components, etc. As a test of the sensitivity to the presence of such objects a 10 cm thick ring of iron is optionally added in the position indicated in Fig. 1. The B field is taken to be 1.4 Tesla/cm and, in order from center, the polarity of the quads is (horizontal) D-F-D for positive particles.

Energy deposition is recorded in the magnet coils ($3.81 \lesssim r \lesssim 5.874$ cm, see Fig. 2) in ring-shaped bins with Δr varying from 0.29 cm (small r) to 0.574 cm, and Δz from 2.7 cm (small z of first quad) to 175 cm. Azimuthal binning is rather coarse: the region $0 < \phi < \pi/4$, as measured in a positive or negative sense from either horizontal or vertical, is divided equally in three parts. This binning is based on the observation that an 8-fold symmetry applies if one assumes identical populations of positive and negative particles in phase space at production, which is not exact but reasonably close. The main exception is that, among energetic (including leading) particles, positives will be more prevalent on the p-side and negatives on the $\bar{p}$-side, but most of these will traverse the low beta quads within the aperture.

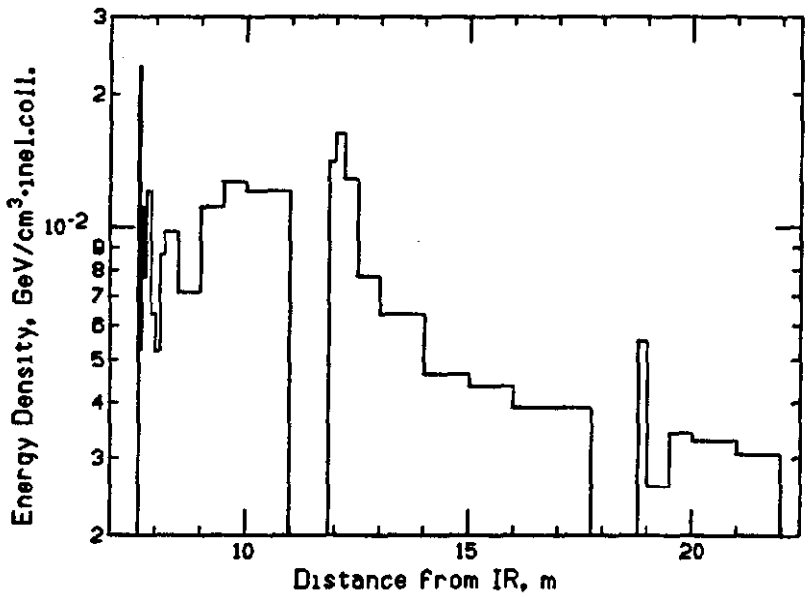

Fig. 3. Energy density in innermost radial region of coils ($3.81 < r < 4.1$ cm) and in azimuthal regions ($0 < |\phi| < \pi/12$) and ($11\pi/12 < |\phi| < \pi$) as a function of distance along the quadrupole string.

The calculated energy deposition as a function of distance along the quad string in the sampling region of the coils located innermost radially and containing the midplane azimuthally, is shown in Fig. 3 for a bare beampipe. It appears that adding 10 cm of iron does make a difference at shallow depth in the first quad. This is illustrated in Fig. 4a where the radial distribution in the slice $0 < z < 2.7$ cm,

averaged over azimuth, is compared for the two cases. However, the difference in energy deposition disappears quickly with depth into the quad, as shown in Fig. 4b for the $7.7 < z < 12.7$ cm region. This suggests that even a relatively thin (~10 cm) collimator, placed directly in front of the first quad, could absorb the excess. The magnitude of the energy densities, approaching 0.03 GeV/(cm^3•inelastic event) for the bare beampipe and 0.1 GeV/(cm^3•inelastic event) with the iron present, are not cause for alarm. To recast these numbers in terms of a quenching limit one can ask for the luminosity needed to attain the nominal 8 mW/g from the Tevatron Design Report.[6] For 0.1 GeV/(cm^3•inelastic event) and assuming $\sigma_{inel} = 80$ mb this corresponds to $5 \cdot 10^{34}$ cm^{-2}sec^{-1}. It should also be recalled that, for fast extraction losses, observed quench limits are somewhat higher than expected from the Design Report (by a factor of ~1.7, though with significant statistical error).

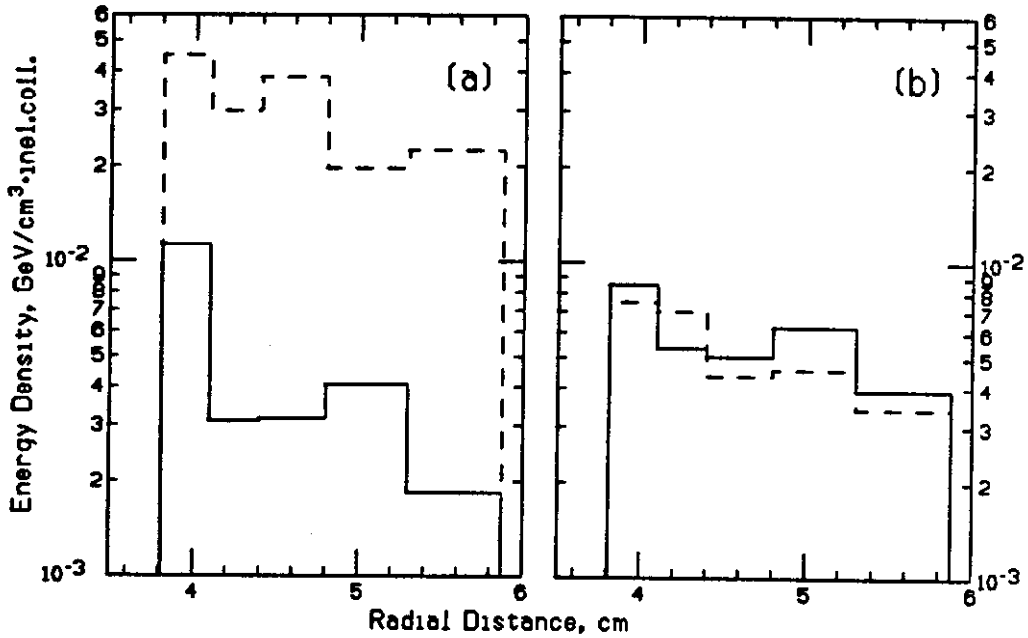

Fig. 4. Energy density as a function of radius at shallow depth in superconducting coils of first quad for a bare beampipe between interaction region and first quad (solid) and with 10 cm extra iron present (dashed) (a) at the beginning of the quad $0 < z < 2.7$ cm, and (b) some 10 cm into the quad ($7.7 < z < 12.7$ cm). The energy density is averaged over ϕ.

Neutrals

The geometry used for simulating energy deposition due to neutrals is shown in Fig. 5. For simplicity the low beta quads are omitted and the dipole string is represented as a continuous magnet with a 754 m bending radius and B field to accomodate 1 TeV protons. The assumed dipole cross section is as in Fig. 6. All material beyond the iron cylinder (representing the stainless steel collars) is neglected since particles observed at these large radii are unlikely to contribute further to the energy deposition at small radii in the coils. Only particles which enter the dipole string within the vacuum chamber are included in the analysis. (For particles striking the front of the first dipole the geometry of Fig. 5 is quite unrealistic.)

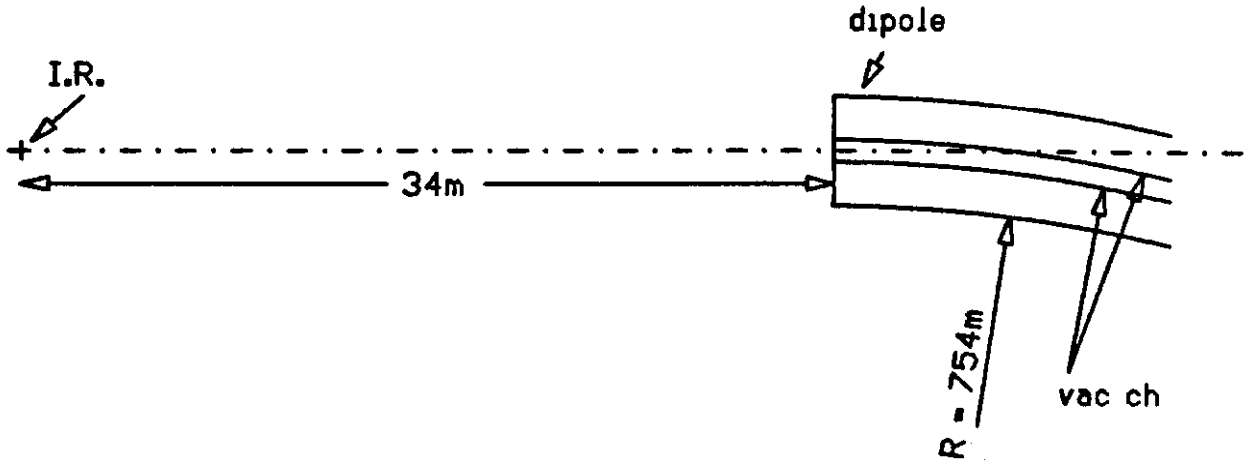

Fig. 5. Schematic geometry (not to scale) to study effects of neutrals and leading particles in dipoles.

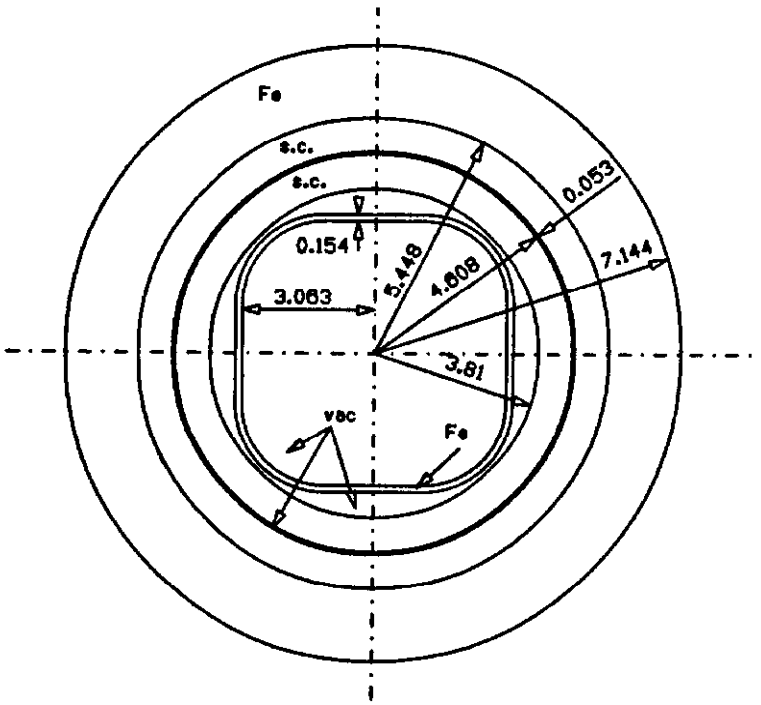

Fig. 6. Cross section of dipole magnet as represented in simulation. All dimensions are in cm.

Energy deposition is recorded in the magnet coils ($3.81 < r < 5.458$ cm) divided radially into three tori, as well as in the vacuum chamber which is 0.154 cm thick and is in the shape of a 'rounded square'. It is easy to imagine this peculiar shape to affect the energy deposition and therefore its shape is faithfully represented in the simulation. The recording bins are azimuthally subdivided into seven unequal wedges with two small regions ($\Delta\phi = 0.2$) centered on the midplane: on the out-side of the vacuum chamber wall for the purpose of recording the neutrals and on the in-side for leading particles. The up-down symmetry of this problem is exploited in the ϕ-binning. Less variation is expected along the z-direction and the bins are sliced into large Δz (100 to 200 cm). To help determine the true maximum energy density in the coils,

rather than an average over some volume bin, the radial energy variation is fitted to an *a priori* selected function (see Ref. 1, further fitting to functions of ϕ and z is not attempted here).

Fig. 7 presents the variation of the maximum energy density in the regions $0 < |\phi| < 0.3$ and $(\pi - 0.3) < |\phi| < \pi$ as a function of z. These regions include the smaller $\Delta|\phi| = 0.1$ bins (about zero and π) which do not show significantly higher energy densities but are statistically noisy. The neutrals peak is indeed observed and is about $2.5 \cdot 10^{-3}$ GeV/cm^3•collision at the maximum. Also from Fig. 7 it can be seen that on the in-side of the dipole (which includes the leading particle contribution) the maximum energy density is about $4.0 \cdot 10^{-4}$ GeV/cm^3•collision. Both these numbers are well below the corresponding value for the low beta quads.

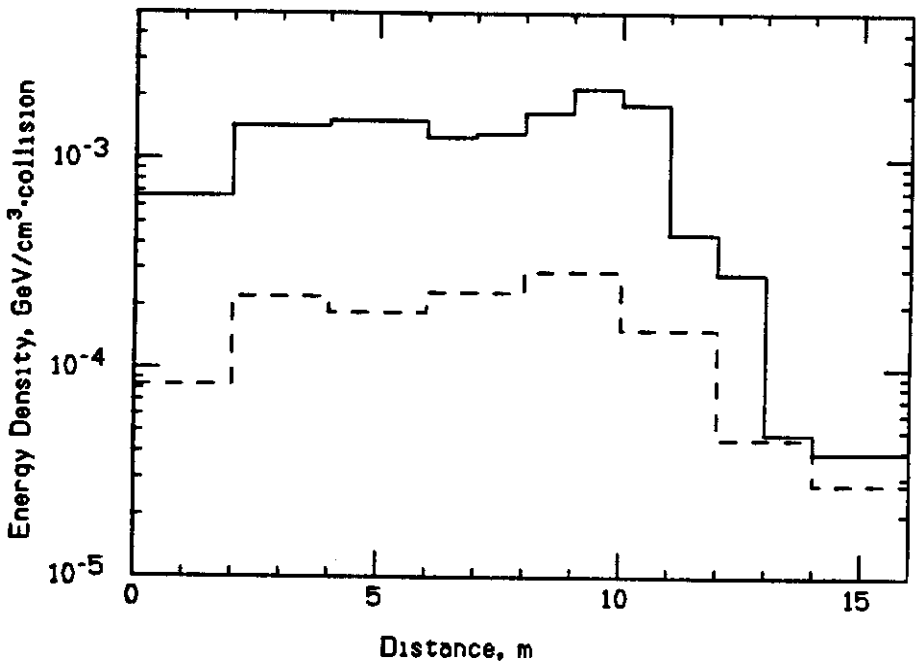

Fig. 7. Estimated maximum energy density in superconducting coil of dipole magnet as a function of z: for $0 < |\phi| < 0.3$, or in-side of ring, where leading particles are expected to strike (dashed) and for $\pi - 0.3 < |\phi| < \pi$, or out-side, where neutrals are intercepted (solid).

ELASTICS

Quenching appears even less probable due to energy deposition by elastics than by the inelastics from comparison with the fast extraction problem. Located much closer to the particle source, and without a protective dogleg, the low beta quads do not appear to be vulnerable at design luminosity. Under similar circumstances in the resonant extraction problem, inelastics would definitely be expected to produce the larger energy densities. The relative number of elastic and inelastic beam losses also favor this conclusion: of all protons intercepting the septum (for typical operation of the Tevatron during extraction) about equal numbers are lost elastically (18.7%) as inelastically (22.9%).[1] (The remainder, mostly particles which suffered only minimal energy loss and scattering in the septum, is extracted in less than three turns.) By comparison for colliding beams $\sigma_{inel} = 80$ mb, $\sigma_{el} = 18$ mb and, for single diffraction,

σ_{sd} = 8.5 mb (per beam, as per usual definition) are working numbers based on extrapolation. Also the collisions take place essentially in the center of mass so that, at least for the pure elastic part, the particles change direction but change their energy very little. In contrast, even purely elastic interactions in the septum are always accompanied by some energy losses of which ionization losses in the tungsten wires is the most significant. There are nevertheless noticeable dissimilarities with the extraction problem. For example, the low beta quads themselves pose severe aperture limitations, raising the possibility that the elastics deposit their energy on top of the inelastic component, estimated above. Moreover, one set of low beta quads could collect elastics from more than one interaction region and from both p and $\bar{p}$ elastics. Since the quads are situated essentially within the detector, such a scenario is likely to be intolerable for many experiments even well below quench threshold and to necessitate, e.g., collimators to be installed. This facet of the problem depends strongly on the experiment being performed and is not further addressed here.

Below it is attempted to delimit the maximum energy deposition by the elastics from inspection of the phase space immediately after scattering. Tracking particles through the lattice and simulating their interactions at a loss point, as in Ref. 1, is not attempted. The three largest contributions to the elastic part are Coulomb scattering, nuclear (hadronic) elastic scattering, and single diffractive particle production wherein one particle becomes a state of low invariant mass while its collision partner (recoil) continues with only small changes in energy and direction.

For the initial phase space of the 900 GeV/c colliding beams it is assumed that $\sigma_y = \sigma_T = 0.032$ mm, $\sigma_x = [\sigma_T^2+\eta^2(\Delta p/p)^2]^{1/2}$ with $\eta = 150$ mm and $\Delta p/p = 1.5 \cdot 10^{-4}$. Distributions of x' and y' are derived using the lattice parameters at the interaction region $\alpha_x = 0.0007$, $\alpha_y = 0.016$, and $\beta_x = \beta_y = 0.5$ m. The x and y coordinates of the collision (x_c,y_c) are normally distributed. Since, for the beams, $\sigma_{y,p} = \sigma_{y,\bar{p}}$ (independent of momentum) it follows that $\sigma_{y,c} = \sigma_{y,p}/\sqrt{2}$. For the x coordinate this must be modified, since $\Delta p/p$ will generally differ for p and $\bar{p}$, and $\sigma^2_{x,c} = \sigma^2_{x,p}\sigma^2_{x,\bar{p}}/(\sigma^2_{x,p} + \sigma^2_{x,\bar{p}})$. Given x_c, the combination $\alpha_x x + \beta_x x'$ is chosen from a Gaussian with $\sigma = \sigma_T$ from which x' follows (ditto for y'). Somewhat arbitrarily (see below) all the Gaussians of the incident distributions are truncated at 3.5σ.

Nuclear Elastic

To simulate the phase space population of the final states of nuclear elastic scattering, the dependence of the cross section on t, the square of the four-momentum transfer, is assumed to follow:

$$\begin{aligned} d\sigma/dt &= A \cdot \exp(16.8t) && 0 \leq |t| < 0.63 \\ &= B && 0.63 \leq |t| < 0.86 \\ &= C \cdot \exp(3.1t) && 0.86 \leq |t| \end{aligned}$$

where A, B, and C are constants fixed by continuity and normalization and t is expressed in $(GeV/c)^2$. This is a parametrization of a theoretical prediction of Gauron et al[7] whose results at lower energy agree quite well with the data. Since selection from the above distribution is very fast no biasing has been applied. Momenta and directions of the final state particles are determined using full kinematics.

As an indication of beam losses, particles scattered into the 'wings' of the phase space are considered lost (after some distance, possibly multiple turns) if $(\alpha_x x+\beta_x x')$ or $(\alpha_y y+\beta_y y')$ falls outside of 5σ. This condition prompted the aforementioned 3.5σ cut on the incident phase space since otherwise even some unscattered incident particles would already qualify as being lost. Fortunately, the scattered phase space is not very sensitive to the precise value of the cut on the incident phase space. Because of the proximity of lab and center-of-mass system, no events with $\Delta p/p$ large enough to be 'lost' are encountered. Obviously, there are no cuts to apply on x and y since these are unchanged in the scattering process. Fig. 8 shows the fraction of particles outside a given limit in $(\alpha_x x+\beta_x x')$ and $(\alpha_y y+\beta_y y')$ as a function of that limit, expressed in units of the corresponding σ of the beam. It is separately indicated whether $(\alpha_x x+\beta_x x')$ or $(\alpha_y y+\beta_y y')$ exceeds the limit (where both qualify the event is sorted with the larger of the two). The fraction of particles outside the 5σ limit is found to be 0.18.

From Ref. 1, a fast loss of $\sim 7 \cdot 10^8$ (elastically scattered) protons striking the last quadrupole at the F49 location suffices to cause it to quench. Scaling this to a corresponding number for continuous operation by the ratio of the nominal design limits[6] for fast and slow losses ($8\ mW \cdot g^{-1}/1\ mJ \cdot g^{-1}$) means that $\sim 6 \cdot 10^9$ p/sec will induce a quench. However, for a luminosity of $L = 10^{31}\ cm^{-2}sec^{-1}$, $\sigma_{el} = 18$ mb, and for 0.18 of the elastics outside of the emittance, only $3.2 \cdot 10^4$ protons per second (and per beam) will be lost ring-wide. For a worst case scenario it should be assumed that all these particles are lost at one location and this could further be multiplied by a factor of four given two interaction regions and since p as well as $\bar{p}$ elastics can, in principle, contribute. Even this scenario leaves an ample margin of safety and the conclusion that, from the viewpoint of magnet quenching, elastics are unlikely to cause any problems. The dependence on the 'loss-limit' of the outgoing phase space, shown in Fig. 8 and somewhat arbitrarily set at 5σ, is not so strong that lowering this limit to 4σ, or even 3.5σ, would alter the conclusion. The scaling procedure above ignores differences in the phase space at production between elastics from p-$\bar{p}$ versus those from the septum as well as possible geometric factors arising at the loss point from striking different magnets in different locations. However, these are very unlikely to overcome the large difference in the numbers of elastics generated in each mode of operation.

Diffractive

The phase space produced by single diffractive recoils is obtained using a parametrization of the cross section, $d\sigma/dtdM^2$, taken from the review of Goulianos.[8] The more detailed algorithm may be found in Ref. 2. Again the full kinematics is applied to derive the parameters of the final state particle. Fig. 9 presents contours of equal particle density in $\Delta p,y'$-space, illustrating the importance of momentum losses in this case. Fig. 10 shows the fraction of particles outside each and any of the $(\alpha_x x+\beta_x x')$, $(\alpha_y y+\beta_y y')$ and Δp limits as a function of the limits expressed in units of the corresponding σ of the incident beam. About 0.66 of the total are outside the 5σ limit, mostly due to momentum losses. From the large Δp encountered here it appears that many of these particles will be lost relatively quickly from the aperture thereby diminishing the likelihood that all are lost at the same location.

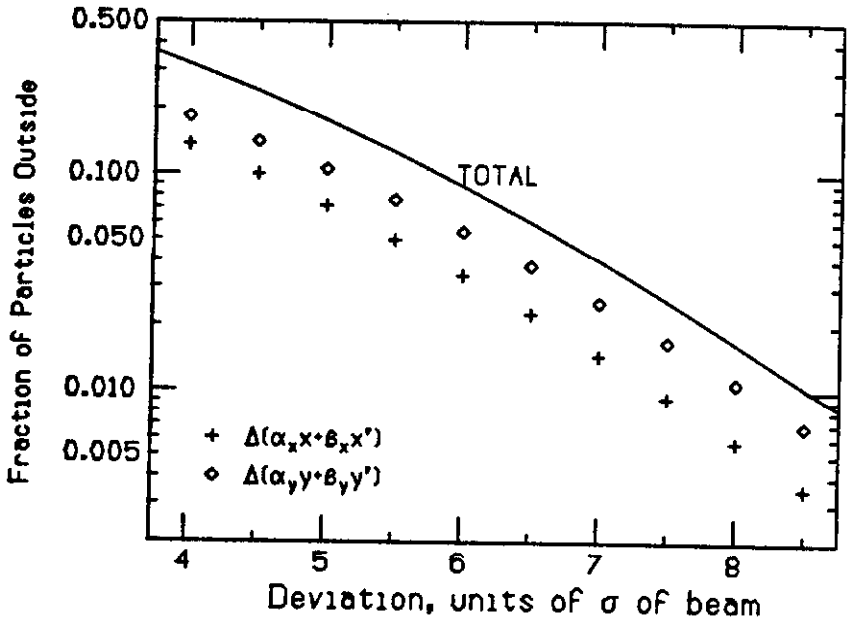

Fig. 8. Fraction of elastically scattered particles outside each of the $(\alpha_x x+\beta_x x')$, $(\alpha_y y+\beta_y y')$ limits and fraction outside either limit (labeled TOTAL) as a function of the limits expressed in units of the corresponding σ of the incident beam.

The argument, made above for the elastics, can be repeated here to demonstrate that single diffractive losses are also expected to be entirely tolerable. For $L = 10^{31}$ cm^{-2}sec^{-1}, $\sigma_{sd} = 8.5$ mb, and for 0.66 of the elastics outside the emittance $5.6*10^4$ protons per second (and per beam) will be lost. Hence no quenching problems are expected even if the combined inelastic, scattering, and diffractive losses from two interaction regions all were to accumulate in one particluar loss location.

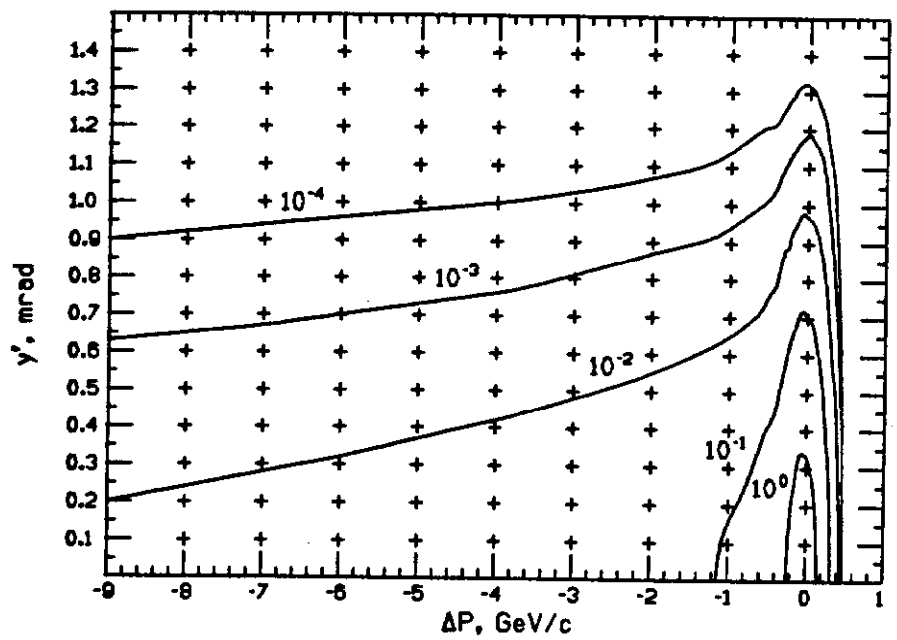

Fig. 9. Iso-density contours in y',Δp -space of single diffractive recoils.

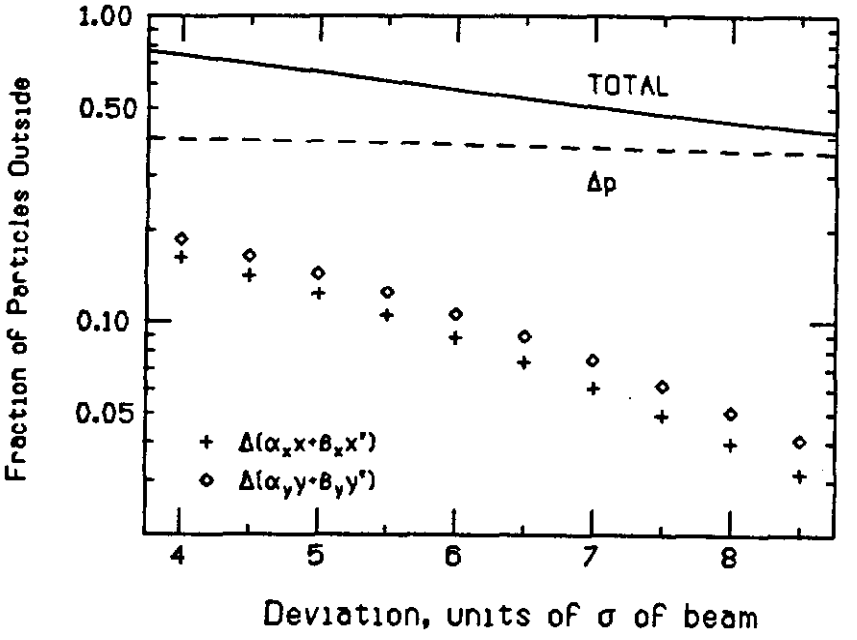

Fig. 10. Fraction of diffractive recoils outside each of the $(\alpha_x x+\beta_x x')$, $(\alpha_y y+\beta_y y')$ and Δp limits, and fraction outside any limit (labeled TOTAL) as a function of the limits expressed in units of the corresponding σ of the incident beam.

Multiple Scattering

Multiple Coulomb scattering incurred during multiple encounters of a particle with members of the opposite beam and summed over multiple turns contributes to a slow growth in beam emittance. While this will also lead to slow losses these are presumably small and not assessed here. The growth in beam emittance, from this and other mechanisms, will shorten the useful beam lifetime and prompt the beams to be aborted well before such losses become significant. Below a brief derivation of the emittance growth is presented and numerically evaluated for beam parameters as listed above for the other elastic mechanisms.

The cross section for Coulomb scattering, $d\sigma/d\Omega \simeq (2\alpha/p\theta^2)^2$, evaluated at 900 GeV and integrated over angle becomes $\sigma_C \simeq 3.1\cdot10^{-10}\theta_{min}^{-2}$ mb, while the mean square angle per scattering is $\langle\theta^2\rangle \simeq 2\theta_{min}^2\ln(\theta_{max}/\theta_{min})$, with θ_{min}, θ_{max} to be determined below. For two Gaussian beams colliding head on the average number of such collisions per crossing, experienced by each particle, is $N_b\sigma_C/4\pi\sigma_x\sigma_y$, where N_b is the number of particles per bunch, and the mean square angle per crossing (at 900 GeV) is $5.0\cdot10^{-36}N_b\ln(\theta_{max}/\theta_{min})/\sigma_x\sigma_y$, with σ_x and σ_y in mm. In view of the log dependence, the derivation of θ_{min}, θ_{max} can be quite sketchy. θ_{min} is obtained by equating $\sigma_C \simeq \pi b^2$ where b is the maximum impact parameter. To estimate b it is assumed the N_b particles are uniformly distributed in a $(2\sigma_x)\times(2\sigma_y)\times(2\sigma_s)$ box, which results in a distance between neighbors of $(8\sigma_x\sigma_y\sigma_s/N_b)^{1/3}$. The half-distance, projected onto the (x, y) plane is a reasonable estimate of b. For σ_x, σ_y as above and for $\sigma_s \simeq 350$ mm this yields $\theta_{min} \simeq 2.1\cdot10^{-14}$. The angle θ_{max} can be chosen as the angle where nuclear and Coulomb scattering are equal which, at 900 GeV, means $\theta_{max} \simeq 3\cdot10^{-5}$. This is still below rms beam angles and, while Coulomb scattering with $\theta \simeq \theta_{max}$ is expected to be relatively rare, the condition $\theta < \langle\theta^2\rangle^{1/2}$ allows for

treating such angles as contributing to beam spreading. With $N_b = 7.4 \cdot 10^{10}$ these numbers combine to yield $\langle\theta^2\rangle \simeq 6.0 \cdot 10^{-21}$ per crossing. If one assumes only two interaction regions contribute, i.e., that the beams are separated elsewhere, then this translates directly into an (instantaneous) rms growth in projected angle of 5 μr per day for each θ_x and θ_y. For $\beta_x = \beta_y = 500$ mm, σ_x and σ_y are expected to grow 2.5 μm per day. This is well below the growth rate, e.g., from intrabeam scattering and is not expected to change the beam emittance materially.

Intermediate Angles

To complete the discussion one should mention beam growth from individual scattering events which fail to expel the particle from the beam ($\theta < \sim 5\sigma$, in the simplistic model used here). For nuclear scattering the fraction remaining within 5σ is estimated at 0.82 for a cross section of 14.8 mb and with an rms angle of $2.1 \cdot 10^{-4}$. For the diffractive component the corresponding cross section is about 2.9 mb and the rms angle is $1.8 \cdot 10^{-4}$. For the Coulomb part the multiple scattering regime ($\theta < \theta_{max}$) must be excluded. The total cross section for the remainder is about 0.35 mb with an rms angle of $5.4 \cdot 10^{-5}$. For all combined, events at these intermediate angles occur at a rate of ~3% of the beam per day.

CONCLUSIONS

It has been shown that energy deposition in the Tevatron superconducting magnets due to particle production and elastic processes in the interaction regions is unlikely to cause any quenching even at luminosities much higher than the design value of 10^{31} cm^{-2}sec^{-1}. The products of inelastic interactions which strike the nearby low beta quads provide the worst scenario in this respect but are not expected to induce a quench unless the luminosity were higher by a factor of ~5000. The peak energy density for the neutral 'beam' striking the dipoles is down further by a factor of 40 to that observed in the low beta quads. For the leading particle contribution the corresponding factor is 250. Though the calculations pertain specifically to the p-$\bar{p}$ option the wide margin of safety implies the same conclusion for the p-p scenario. For the low beta quads this is confirmed by more detailed calculations, not reported here, which show the maximum energy density to be about the same for both options.

Elastically scattered particles are analyzed both in terms of losses and of a slow beam growth (2.5 μm/day at the interaction region). While detailed calculations of the energy deposition are not performed here, a comparison with earlier such calculations, performed in connection with fast extraction losses, plus the 'worst case' assumption that all elastic losses occur on the same magnet, lead again to a margin of safety of ~5000. However, aside from quenching considerations, a significant loss of the elastics on the low beta quads could be unacceptable to nearby experiments at much lower luminosties. The separation of the elastically scattered particles into beam growth and beam loss, while not entirely realistic, has the virtue of convenience and avoids double counting. More detailed treatments, if need be, should be done in connection with other unavoidable mechanisms of beam loss and growth.

My thanks to C. Ankenbrandt and M. Harrison for suggestions and discussion. K. Koepke and E. Malamud furnished the needed design information. S. Qian provided the cross section fit and kinematics program for nuclear elastic scattering.

REFERENCES

[1] A. Van Ginneken, D. Edwards, and M. Harrison, Quenching Induced by Beam Loss at the Tevatron, in High Energy Hadron Colliders, A. Chao, H. Edwards, and M. Month, Eds., American Institute of Physics, New York (1987).

[2] A. Van Ginneken, Phys. Rev. D **37**, 3292 (1988).

[3] J. Ranft et al, SSC-Report SSC-149 (1987).

[4] A. Van Ginneken, Fermilab Report FN-272 (1975).

[5] 'Low' beta quads refers to the purpose of these quads to provide a low beta at the interaction region even though this implies a large value of beta at the quads' own location.

[6] Report on the Design of the FNAL Superconducting Accelerator, F. T. Cole et al, Eds., Fermilab (1979).

[7] P. Gauron, B. Nicolescu and E. Leader, Phys. Rev. Lett. **54**, 2656 (1985).

[8] K. Goulianos, Phys. Rep. **101**, 169 (1983).